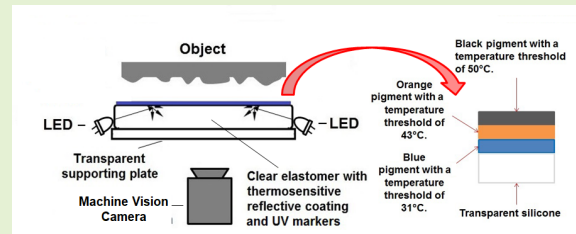


# HaptiTemp: A Next-Generation Thermosensitive GelSight-like Visuotactile Sensor

Alexander C. Abad, *Member, IEEE*, David Reid, *Member, IEEE*,  
and Anuradha Ranasinghe, *Member, IEEE*

**Abstract**—This study describes the creation of a new type of compact skin-like silicone-based thermosensitive visuotactile sensor based on GelSight technology. The easy integration of this novel sensor into a complex visuotactile system capable of very rapid detection of temperature change (30 °C/s) is unique in providing a system that parallels the withdrawal reflex of the human autonomic system to extreme heat. To the best of authors' awareness, this is the first time a sensor that can trigger a sensory impulse like a withdrawal reflex of humans in robotic community. To attain this, we used thermochromic pigments color blue, orange, and black with a threshold of 31 °C, 43 °C, and 50 °C, respectively on the gel material. Each pigment has the property of becoming translucent when its temperature threshold is reached, making it possible to stack thermochromic pigments of different colors and thresholds. The pigments were air-brushed on a low-cost commercially available transparent silicone sponge. We used MobileNetV2 and transfer learning to simulate tactile preprocessing in order to recognize five different objects. The new thermosensitive visuotactile sensor helped to achieve 97.3% tactile image classification accuracy of five different objects. Our novel thermosensitive visuotactile sensor could be of benefit in material texture analysis, telerobotics, space exploration, and medical applications.

**Index Terms**—thermochromic pigment, visuotactile, thermosensitive



## I. INTRODUCTION

ALTHOUGH psychologists often state that vision is the main way humans obtain information from the environment [1], when visual perception is impaired, haptic perception is the natural recourse [2]. Even if vision is not impaired, the sense of touch often works in conjunction with visual perception. In this paper, this combination of vision and touch is termed *visuotactile*. Research into visuotactile perception dates back to the 18th century [3] and is increasingly becoming a multidisciplinary field of study not only by philosophers and psychologists but also by engineers, technologists, and roboticists in the fields of haptics, tactile robotics, machine vision, and artificial intelligence [4]–[7].

A visuotactile sensor is similar to a flexible mirror that converts physical contact or pressure distribution on the reflective layer into a tactile image that can be seen or captured by a camera [7]. Tactile images produced by a visuotactile sensor

can be analyzed in real-time to study tactile forces such as slip, shear, and torque and can also be recorded and stored for further processing and analysis. These tactile images can be used for many purposes such as metrology, 3D image reconstruction, and object recognition or classification. The earliest known visuotactile sensor was not used for the hand but for the foot. It is known as the pedobarograph developed by Chodera et al. in the 1950s to 1970s [8]–[10]. Pedobarograph uses elastic foil on top of a transparent plate with a camera on the other side on which a human can stand or walk. The plate is illuminated on its side, and the light is diffused by Total Internal Reflection (TIR). Foot pressure distribution as the foot presses the elastic foil creating different light intensities reflected through the plate can be recorded for posture and gait analysis [10], [11].

The first miniature pedobarograph-like visuotactile sensor fitted on a robotic arm was reported during the 1960s at the MIT lab [12]. Two prototypes were developed. The first one is by Kappl in 1963 that used a polyurethane rubber as photoelastic material for a pattern generator similar to a polariscope. Moreover, in 1966, Strickler and Sheridan introduced a visuotactile sensor with a flexible mirror that produced high contrast optical stress patterns and was used for a remote manipulator.

During the 1980s, high-resolution visuotactile sensors were developed. Schneider and Sheridan from MIT [13] demonstrated in 1984 an optical touch sensor that has a flexible

This work was supported by the Department of Science and Technology (DOST), Engineering Research and Development for Technology (ERDT), Philippines. (Corresponding author: Alexander C. Abad.)

Alexander C. Abad is with the Faculty of Science, School of Mathematics, Computer Science, and Engineering, Liverpool Hope University at Hope Park, Liverpool L16 9JD, U.K., and also with the ECE Department, Gokongwei College of Engineering, De La Salle University, Manila 1004, Philippines (e-mail: abada@hope.ac.uk).

David Reid and Anuradha Ranasinghe are with the Faculty of Science, School of Mathematics, Computer Science, and Engineering, Liverpool Hope University at Hope Park, Liverpool L16 9JD, U.K. (e-mail: reidd@hope.ac.uk; dissana@hope.ac.uk).

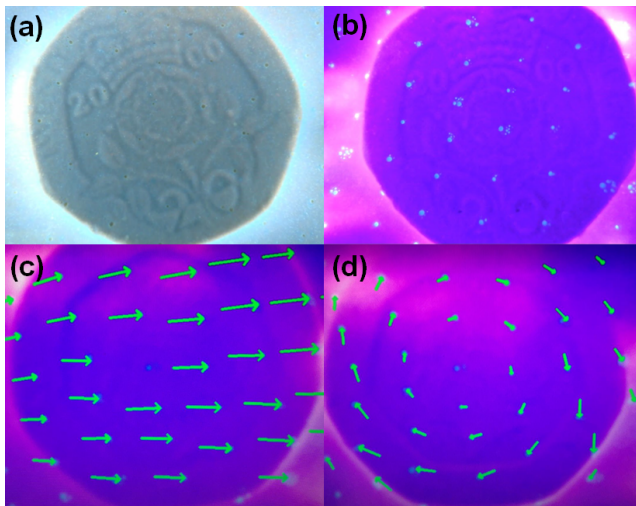


Fig. 1. Activation of thermosensitive GelSight-like sensor with UV markers and thermochromic reflective layer for mechanical response; (a) UV LEDs off, (b) UV LEDs on, (c) flow vector arrows showing shear force [46], and (d) flow vector arrows showing torque or twisting force [46].

material with reflective coating and uses optical fiber technology. This optical touch sensor has 2100 sensitive points per square inch resolution. On the other hand, Tanie et al. from Japan in 1984 developed a small-high resolution pedobarograph-like tactile sensor using pressure-optical conversion technique, and has a 32 x 16 phototransistor array [14]. Tanie et al. improved their design using Charged Coupled Device (CCD) camera and can be used to capture the precise profile of 3D objects [15]. In 1988, Begej developed another CCD camera-based visuotactile sensor that focused not only on planar but also on finger-shaped visuotactile sensors for robots [16]. Begej's sensors operate on TIR to produce a gray-scale image of the contacted object.

Tanie et al. developed three versions of finger-shaped visuotactile sensors during the 1990s. Different hemispherical shapes with diameters of 54 mm [17], 32 mm [18], and 20 mm [19] were developed. Moreover, during the mid-1990s, Ohka et al. developed 3-axis visuotactile sensors that use different kinds of feeler arrays to detect 3-axis force components [20], [21]. In 2008, A biologically inspired visuotactile sensor, known as TACTIP [22], with artificial papillae similar to column feelers was developed in Bristol Lab, UK.

Instead of using feelers, the use of markers was introduced in the visuotactile sensors at the start of the 21st century. A human-fingertip-like sensor with deformable membrane and skin markers was introduced in Harvard Robotics Lab in 2000 [23]. A year later, Tachi Lab in Japan introduced a visuotactile sensor, known as the GelForce, that can measure 3D vector distribution. GelForce has a transparent elastic body with two layers of bead marker matrices (red and blue layers) and a camera at the bottom. The applied force is calculated based on the movements of the markers captured by the camera [24]. A finger-shaped GelForce with a thermosensitive layer was reported in 2011 [25], [26]. In 2019, Sferenza et al. developed a visuotactile sensor with fluorescent green spherical markers randomly embedded in the flexible material

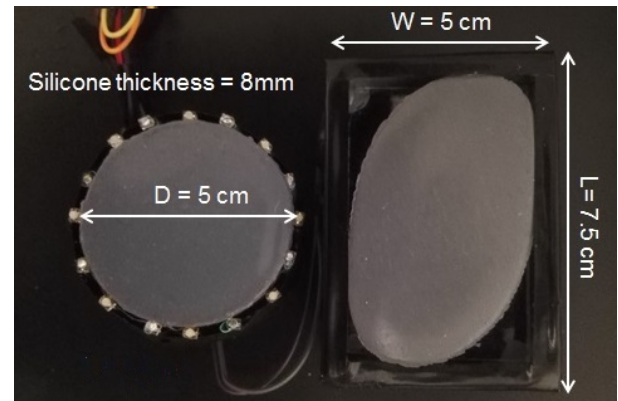


Fig. 2. Different silicone shape configurations.

to analyze tactile forces inferred from the movement of the markers [27]. Moreover, Lin and Wiertelowski introduced in 2019 a visuotactile sensor with embedded semitransparent two-color dye markers instead of beads inside the flexible material to analyze tactile forces from gel deformation when contacted by an object [28].

A visuotactile sensor that fuses vision and tactile sensing to a high degree of inter-modal fusion was developed by Johnson and Adelson in 2009, known as the GelSight sensor. It is a high-resolution miniature pedobarograph-like sensor capable of capturing microscopic surface geometry as small as 2 microns with sensitivity and resolution exceeding that of the human fingertips [29]. The GelSight sensor is an ideal visuotactile sensor because of its high spatial resolution in vision [30] and high sensitivity in tactile [31]. This visuotactile sensor has proven its worth in a wide range of applications from haptics, robotics, and computer vision. A comprehensive literature review on visuotactile sensors with emphasis on GelSight sensor is reported in [7].

The original GelSight sensor of 2009 was introduced as a “retrographic sensor” [29] – a flexible material with a sensitive reflective coating on top of a transparent plate on which a tactile image of the contacted object can be seen at the back of the supporting plate. This retrographic sensor with controlled lighting and camera was used to get high-resolution 3D image reconstruction for metrology and microgeometry analysis. It was Jia et al. who introduced the name “GelSight sensor” [32] to the whole visuotactile sensor setup presented by Johnson and Adelson in 2009.

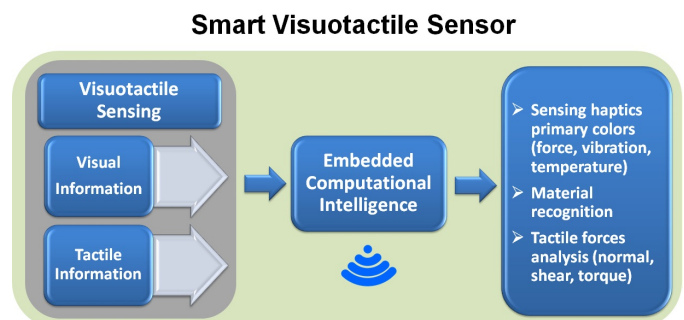


Fig. 3. Capturing visuotactile information.

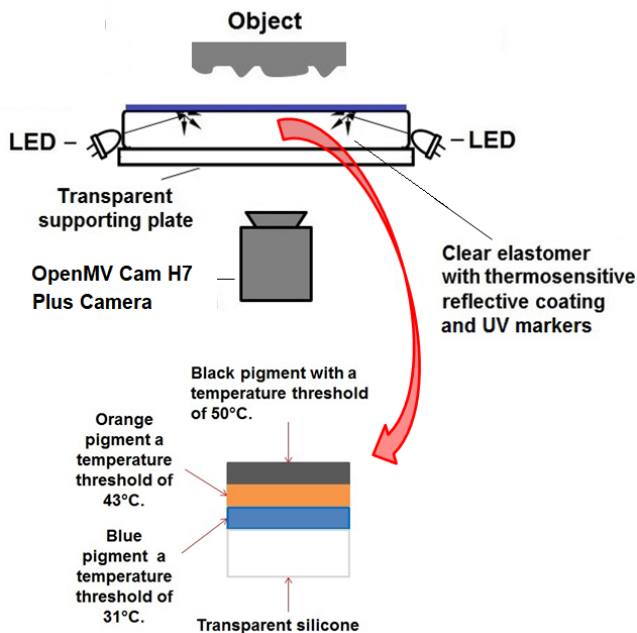


Fig. 4. The thermosensitive visuotactile sensor structure is similar to GelSight sensor structure but has a flexible material with thermosensitive reflective coating and uses a machine vision camera for on-board tactile image classification and analysis.

Though the first application of the GelSight sensor is in metrology, especially in the 3D image reconstruction, the inventors reported that it could be used as a skin model, and a tactile sensor for robotics. In 2014, Li *et al.* first used the GelSight sensor as a tactile sensor of a robotic hand to localize and manipulate small parts [33]. GelSight sensor applications can be categorized into three major groups: 1) tactile 3D image reconstruction for metrology, 2) tactile/haptic sensing, and 3) tactile image recognition or classification. The majority of reported GelSight sensor applications are in the field of tactile sensing in robotics, and tactile image recognition or classification [7]. This study will only focus on our GelSight-like visuotactile sensor for tactile sensing and tactile image recognition applications.

Current GelSight sensors are created in the lab and can be divided into two categories: with and without permanent grid dots or markers [34]. Permanent markers in the form of dots or triangles on the reflective coating of the GelSight sensor were introduced by Yuan in 2014 [35]. The motion of markers as the gel deforms when contacted by an object can be tracked using an optical flow algorithm or flow vector arrows to deduced normal force, shear force, and slip [35], [36]. GelSight sensor used in the measurement of microgeometry [30], surface texture [29], lump detection [32], and tactile mapping and localization [37] do not have grid dots or permanent markers while GelSight sensor with permanent markers was utilized in the measurement of shear and slip [30], [36], [38]–[41].

In most recent GelSight related work [36], [42]–[44], with markers could become an obstruct in the image recognition/classification. The permanent markers in the reflective coating of the GelSight sensor could be treated as noise in 2D image processing that might conceal some important image

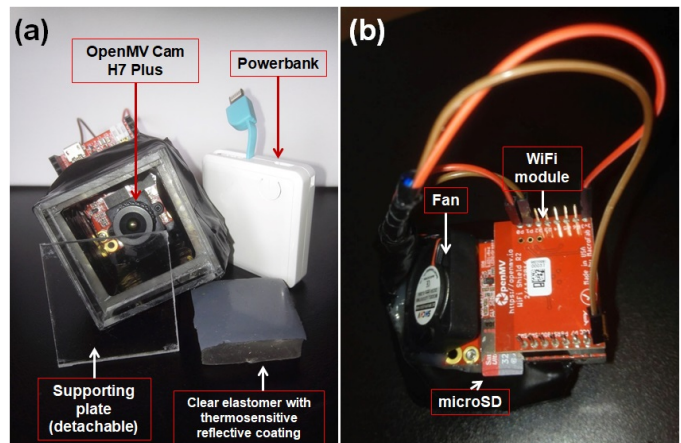


Fig. 5. Thermosensitive visuotactile sensor using OpenMV Cam H7 plus with WiFi module: (a) front view and (b) bottom view.

features that are helpful for object recognition [7]. Permanent markers might negatively affect some important 2D image features, especially if these markers are more significant than the image features [36]. This issue might be observed in the images presented in [42]–[44] where the GelSight sensor with permanent markers was used in textile characterization and classification. Moreover, if the application is in metrology, the capability of the GelSight sensor to measure contact surfaces heightmap is affected by the density of permanent markers [40]. To address the issue with permanent markers, we can use UltraViolet (UV) markers. In our previous studies [34], [45], we demonstrated that UV markers could be incorporated into the gel, as shown in Fig. 1. By using UV LEDs, we can make the UV markers visible. Without UV light, the UV markers are invisible and the retrographic image from the GelSight-like sensor can be used in image recognition and classification as shown in Fig. 1(a). When the UV LEDs are on, the UV markers become visible as shown in Fig. 1(b), and we can visualize slip or shear, and torsion using an optical flow algorithm and vector arrows to track these markers as shown in Fig. 1(c) and Fig. 1(d). The use of switchable UV markers mitigates the negative effects of permanent markers that may hide some important image features that might be helpful for object classification through image processing, especially if these markers are bigger than the image features. Our switchable UV markers helped us to create a unified visuotactile sensor that can be used to study tactile forces from mechanical deformation of the gel, and tactile image recognition/classification using one elastomeric slab [34].

Moreover, the curing time in creating a clear silicone gel can be long in laboratory conditions. Therefore, in our previous studies [34], [45], [46], we managed to come up with some alternatives for the above drawbacks. We reported how to create a low-cost Gelsight sensor using a commercially available cosmetic sponges, as shown in Fig. 2, that come in different shapes and sizes. We can cut the silicone sponge to any size we need using a sharp blade or scalpel. Long hours of curing time of about six or seven hours [35], the need for vacuum pump for degassing [35], [47]–[49] to remove bubbles within a gel, and the complex process related to making clear

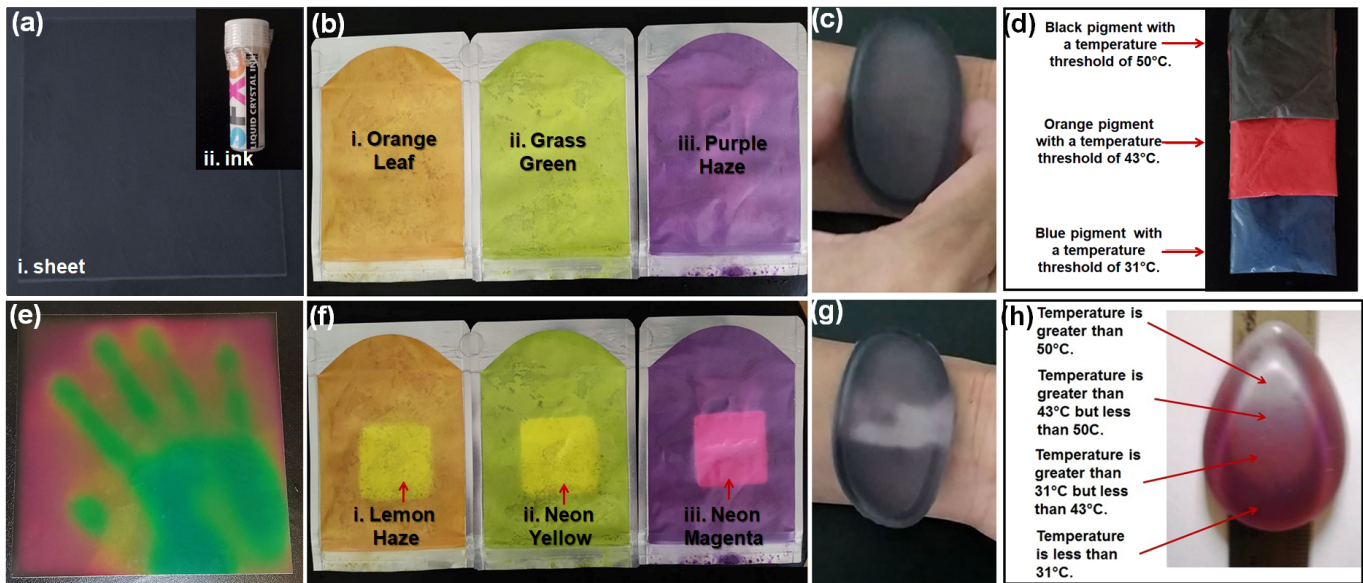


Fig. 6. Thermochromic materials. (a). Inactive SFXC thermochromic liquid crystal thermocolor sheet [53], (a)ii. Sprayable SFXC liquid crystal ink [54], (b) inactive color-changing thermochromic pigment trial pack [55], (c) a black thermochromic pigment, (d) three different thermochromic pigments from HALI CHEMICAL CO.,LTD. [56], (e) SFXC thermochromic liquid crystal thermocolor sheet [53], (f) thermochromic pigments in Fig. 6(b) with 27°C threshold were activated, (g) the human body temperature which is above 31°C activates the thermosensitive pigment making it white to semi-transparent. The rest of the color changes can be found in a test video here [57], and (h) The actual thermosensitive visuotactile sensor subjected to different temperature gradients using a metal ruler heated at one end.

elastomer slab can be skipped using commercial off-the-shelf (COTS) clear silicone cosmetic sponge with Shore A values of 2.5 and 7 as reported in [45]. The 8 mm thickness of COTS clear silicone we used in this study might be considered thicker than the generally 1 mm to 2 mm used in current GelSight sensor structures [35] but might have a good advantage in sensing normal force because it has more room for downward pressure. The COTS elastomer we used is thinner compared to the original GelSight's elastomer presented in this video [50].

The tactile or haptic sensing capability of the GelSight sensor can be further improved to make it a stand-alone fully Haptic Primary Color visuotactile sensor; this is illustrated with a block diagram shown in Fig. 3 and the schematic diagram of our prototype as shown in Fig. 4 that shows thermochromic material to measure temperature, UV markers for mechanical deformation (force) tracking, and elastic gel or elastomer to measure vibration. Our actual prototype is shown in Fig. 5. Tachi et al. theorized that haptics, like light, can be reduced to three components and named them as Haptic Primary Colors (HPC) known as force, vibration, and temperature corresponding to tactile and thermal sensation receptors [51]. GelSight sensor has been used in metrology, object or texture recognition or classification, and tactile forces analyses [6], [7], [29], [44]. It has been reported that aside from force, GelSight sensor can sense vibration such as human pulse [50]. We demonstrated a pilot study of a compact and unified visuotactile sensor made from a commercially available cosmetic sponge with UV markers and thermochromic pigments on the reflective layer to sense force, vibration, and temperature [46]. In this, the mechanical deformation of the gel can be tracked using UV markers and an optical flow algorithm to sense tactile forces. Using this system, we could measure the frequency using a blob detection algorithm and

count the number of blobs produced by a contacted object per unit time. Moreover, we demonstrated that we could easily sense temperature using the hue value by using different colors and layers of thermochromic pigments with varying thresholds of temperature on the reflective coating.

This thermosensitive visuotactile sensor is the first monolithic elastomer temperature sensor and can be used to infer tactile forces based on the mechanical deformation of the gel. Moreover, none of the visuotactile sensors have a different thermosensitive reflective coating to study rapid temperature change (30°C/s), which can mimic the rapid temperature changes equivalent to the withdrawal reflex of humans. Using an embedded OpenMV Cam H7 Plus [52] camera allowed us to easily implement sophisticated machine vision that far exceeds the capabilities of conventional passive camera-based systems.

In this paper, we propose three novel improvements to the current GelSight sensor as follows:

- 1) *thermosensitive reflective coating for temperature sensing using different layers of thermochromic pigments with different colors and temperature thresholds;*

Unlike the thermosensitive liquid sheet that is not elastic used in finger-shaped GelForce [25], [26], we used different layers of thermochromic pigments with different colors and thresholds painted as the reflective coating of elastic clear silicone to make a low-cost GelSight-like sensor with temperature sensing capability. The use of pigment makes the whole reflective layer thermosensitive and compliant as the gel deforms as shown in Fig. 1.

- 2) *Recognize tactile images using machine vision by OpenMV Cam H7 Plus camera; and*

Current GelSight sensors use an ordinary passive camera such as a webcam and raspberry pi camera. All the image

processing with or without the help of artificial intelligence was done using a desktop or laptop computer. Thus, we present a more compact and unified stand-alone solution in this study using OpenMV Cam H7 Plus camera for on-board tactile image recognition. The OpenMV Cam H7 Plus is a small, low-power microcontroller board that allows you to implement applications using machine vision in the real world easily. It can be programmed in high-level Python instead of C/C++, making it easier to deal with the complex outputs of machine vision algorithms and work with high-level data structures. This camera allows us to take pictures and video on external events or execute machine vision algorithms to figure out how to control its Input/Output (I/O) pins. This camera has a built-in STM32H743II ARM Cortex M7 processor capable of Edge Impulse integration for easy training of TensorFlow Lite Models. TensorFlow Lite allows us to do image classification and segmentation models on board the OpenMV Cam. With TensorFlow Lite support, we can easily classify complex regions of interest in view and control I/O pins [52].

### 3) wireless connectivity.

We also incorporated a WiFi module for wireless connectivity, making it untethered and portable. The actual cube prototype used in this study with a side length of 4 cm as shown in Fig. 5.

This paper is structured as follows: design considerations are discussed in section II, evaluation of results in section III, followed by conclusion and recommendation in section IV.

## II. DESIGN CONSIDERATIONS

The visuotactile sensor we developed is based on GelSight sensor technology that has four essential components as defined by Jia *et al.* [32]: 1) clear elastomer with a reflective coating on one side, 2) transparent plate support for the elastomer, 3) controlled and uniform lighting usually from Light Emitting Diodes (LED), and 4) camera to capture the retrographic image [29], [30]. Instead of using ordinary pigments, such as bronze flake or aluminum flake pigment for the semi-specular coating, and fine aluminum powder for the matte coating as discussed in [36], we introduced thermochromic pigments to make the reflective coating capable of sensing temperature. Moreover, instead of using an ordinary camera or webcam, we used machine vision OpenMV Cam H7 Plus camera for tactile image recognition within the sensor module. Details on these novel improvements in the reflective coating and the use of machine vision camera are discussed in the following sections. The schematic of our thermosensitive visuotactile sensor structure is shown in Fig. 4.

### A. Elastomer slab with a thermosensitive reflective coating and UV marking

In our previous studies [34], [45], as well as in the previous section of this paper, we discussed the advantages of using a commercially available cosmetic sponge. We also demonstrated the use of switchable UV markers that can be turned on or off using UV LEDs. However, our previous studies have been limited to study object recognition and tactile forces visualization using flow vector arrows. In this

study, for the first time in a visuotactile sensor like GelSight sensor is introduced with thermosensitive reflective coating using thermochromic pigments that change colors when a certain temperature threshold is reached.

There are different types of thermochromic materials, as shown in Fig. 6. Materials in the top row are inactive state of (a) thermochromic liquid crystal, (b) color-to-color thermochromic pigments, (c) color-to-translucent thermochromic pigment, and (d) multiple color-to-translucent thermochromic pigments with different temperature thresholds as shown in Fig. 6(a), Fig. 6(b), Fig. 6(c), and Fig. 6(d), respectively. The bottom row of Fig. 6 are the activated state of thermochromic liquid crystal sheet, color-to-color thermochromic pigments, color-to-translucent thermochromic pigment, and multiple color-to-translucent thermochromic pigments with different temperature thresholds as shown in Fig. 6(e), Fig. 6(f), Fig. 6(g), and Fig. 6(h) respectively. Thermochromic materials can be in the form of thermochromic liquid crystals sheet [53] or sprayable ink [54], as shown in Fig. 6(a)i. and Fig. 6(a)ii. respectively. Thermosensitive liquid crystal sheets were used by finger-shaped GelForce [25], [26]. Thermochromic liquid crystals are thermosensitive materials that are water-based solutions and cannot be dissolved in solvents [54]. Therefore, we used thermochromic pigments because they can be dissolved in silicone solvent, making it possible to spray on the clear silicone gel material using an airbrush. There are two types of commercially available thermochromic pigments. The first type changes from one color to another color [55] as shown in Fig. 6(b) with an activated state as shown in Fig. 6(f). The orange leaf color of Fig. 6(b)i. will turn into a lemon haze color when activated, as shown in Fig. 6(f)i. The grass green color of Fig. 6(b)ii. will turn into a neon yellow color when activated, as shown in Fig. 6(f)ii. The purple haze color of Fig. 6(b)iii. will turn into a neon magenta color when activated as shown in Fig. 6(f)iii. The second type of thermochromic pigment changes from its base color to translucent or semi-transparent when it reaches the thermal threshold, as shown in Fig. 6(c) and its activated state as shown in Fig. 6(g). Binary temperature sensing of either hot or cold can be demonstrated using a single layer of thermochromic pigment. In this example, a black pigment with a 31°C temperature threshold turns white to translucent whenever the sensor is in contact with the human body.

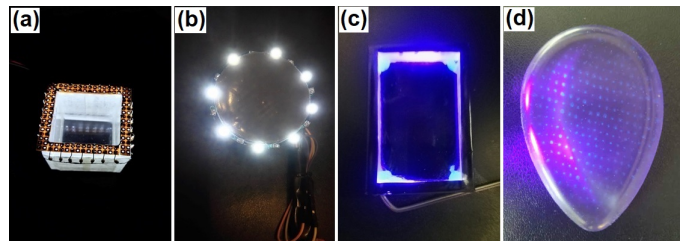


Fig. 7. LED lighting for the sensor used 1.8mm ultra-bright white and UV LEDs arranged alternately: (a) white LEDs are on illuminating a cube box configuration with a side length of 4 cm, (b) white LEDs are on in a circular configuration, (c) 1.8 mm UV LED's are on illuminating a rectangular box, and (d) UV Markings on the reflective coating become visible in the presence of UV light.

Because of the translucent property of the second type of thermochromic pigments when its the temperature threshold is reached, different pigment layers of different colors with increasing thermal thresholds can be put on top of the other to sense different temperature ranges as shown in Fig. 6(d) and Fig. 6(h) respectively.

In this study, we used three different thermochromic pigments bought from HALI CHEMICAL CO.,LTD. [56]. We created a sensor with three different layers of thermochromic pigments with different thresholds, as shown in Fig. 6(d). We used blue color with a temperature threshold of 31°C closest to the clear silicone slab, then an orange pigment with a temperature threshold of 43°C on top of blue pigment, followed by a black pigment with a 50°C temperature threshold. Each thermochromic pigment becomes semi-transparent whenever its temperature threshold is reached, making it possible to make a gradient change in color. When the threshold of blue pigment is reached, it becomes transparent to show the color of orange on top of it. The same is the case when the temperature exceeds the threshold of orange that it becomes black. The layering order of increasing temperature threshold from the clear gel is very important to sense a wide range of temperatures. When our sensor with different layers of thermochromic pigments was placed on top of a metal ruler that was heated at one end, the sensor shows different colors, as shown in Fig. 6(h), showing a gradient temperature of the metal ruler. Please note: this is just a visual representation of temperature sensitive colors. This feature has been carried out to design our cover temperature sensitive visuotactile sensor. The automation is presented with characteristic curves to demonstrate temperature gradient in section III. The rest of the color changes can be found in a test video here [57].

## B. Lighting

Physical contact to image conversion is an important aspect of the visuotactile sensor. There is a need for controlled and uniform lighting to capture tactile or texture image on the flexible material through the deformation of the reflective coating when contacted by an object. Typical structures and features in tactile image sensors employing a camera with discussions about the conversion method from physical contact to light signal have been discussed in [58].

In this study, we used 2 mm clear acrylic plates as our waveguides to produce lighting similar to the structure of fingertip GelSight presented in [33]. A cubic structure used in this study is shown in Fig. 7a. Moreover, round and rectangular configurations that were made to accommodate other silicone shapes and sizes without cutting the gel are shown in Fig. 7(b) and Fig. 7(c), respectively. We mounted alternating 1.8 mm white and UV LEDs in all the structures. White LEDs are on in Fig. 7a and b, while UV LEDs are on, as shown in Fig. 7c. Invisible UV markings on the reflective coating become visible in the presence of UV light, as shown in Fig. 7d.

White LEDs and UV LEDs can be switched on or off manually using a simple switch or electronically using a microcontroller. When our prototype is mounted on a robotic arm or mounted remotely, the switching of white or UV LED's

can be done electronically. The OpenMV Cam H7 Plus camera that we used in this study has a built-in image processor and General-Purpose Input/Output (GPIO) pins that can be used for LED control.

Since this study focuses on haptic sensing and tactile image classification, we have not used multicolor LEDs like the original GelSight sensor for differentiated illumination in getting the heightmap for 3D image reconstruction. In the near future, we will explore the possibility of getting the heightmap of a tactile image using one color lighting because according to Yuan [35], there are two ways to get differentiated illumination direction using a static camera: 1) switching different LEDs positioned at different locations and take separate pictures of the same scene, and 2) using multicolor LEDs simultaneously and take a single picture; the reflection of different color LEDs can be known by taking different channels of the color image.

## C. Machine Vision Camera

We define passive camera as a device that captures photos or videos without any image processing within the sensor module. Webcam and raspberry pi camera are passive cameras. Prototypes from previous studies used Logitech C310 and C270 webcams, while the Gel-Slim [39] configuration used raspberry pi camera.

In contrast with a passive camera, a machine vision camera has a built-in GPIO pins and embedded image processor with machine vision library that can do image processing and image classification within the camera module without the need of external computer. We can make a stand-alone GelSight-like sensor capable of tactile forces analysis and tactile image classification by replacing the webcam with a machine vision camera. There are so many machine vision camera modules available in the market, such as Sipeed MAix Go [59], M5StickV [60], Kittenbot Koi AI [61], Jevois [62], Huskylens [63], Google AIY vision kit [64], OpenCV AI Kit (OAK) [65], and OpenMV Cam H7 Plus [52]. We have chosen to use the OpenMV Cam H7 Plus, as shown in Fig. 5a, because of its small size and has WiFi module that can be easily attached to it as shown in Fig. 5b. To the best of our knowledge, this is the first GelSight-like sensor that uses a machine vision camera. The OpenMV Cam H7 Plus lens focus can be adjusted manually by rotating the lens cover. Unlike in the previous GelSight sensor prototypes, our visuotactile sensor, as shown in Fig. 5, has a detachable supporting plate for the silicone material so that the machine vision camera can be exposed. Therefore, the camera itself can be used for usual applications in image capture, image feature analysis, and pattern recognition when the visuotactile sensor gel is detached. This modular feature of our visuotactile sensor adds to the novelty and flexibility in our use of a machine vision camera.

## D. Software

The OpenMV integrated development environment (IDE) that uses MicroPython programming language is the premier IDE for use with OpenMV Cam. It features a powerful text editor, debug terminal, and frame buffer viewer with a

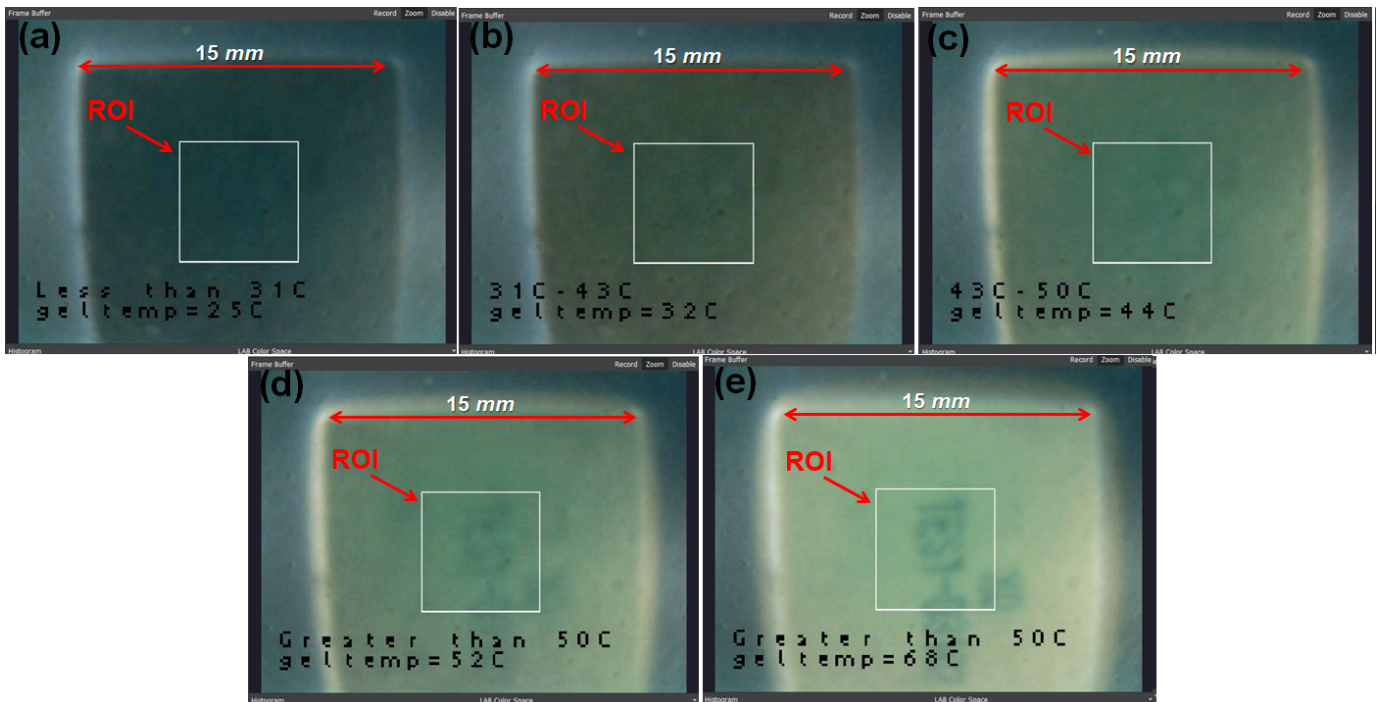


Fig. 8. Temperature sweep test results. (a) Less than  $31^\circ\text{C}$  pigment threshold is dark blue. (b) The blue pigment becomes transparent to show the orange pigment on top of it. (c) When  $43^\circ\text{C}$  threshold of the orange pigment is reached, it becomes transparent to show the black pigment on top of it. (d) When the topmost pigment that has the highest threshold of  $50^\circ\text{C}$  is activated, it starts to become transparent. (e) When the TEG temperature is way beyond the highest pigment threshold of  $50^\circ\text{C}$ , the reflective coating of our sensor becomes transparent enough to show the markings on TEG. The rest of the color changes can be found in a test video here [57]

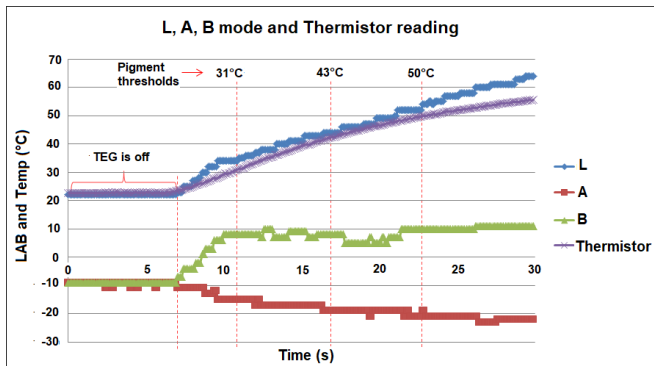


Fig. 9. L,A,B mode values and thermistor reading in the temperature sweep with 23 seconds elapse time covering all the pigment thresholds.

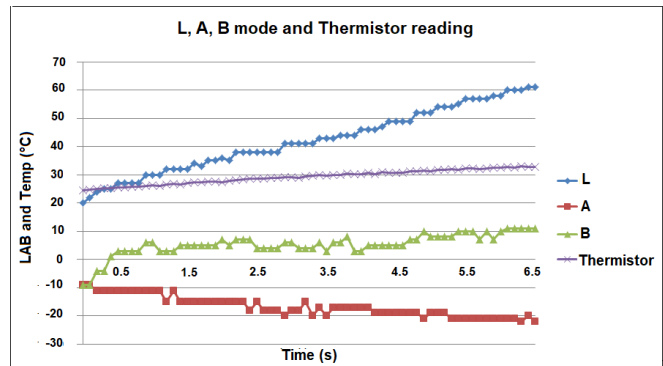


Fig. 10. HaptiTemp vs thermistor response. LAB mode values vs thermistor reading during the 6.5 seconds temperature sweep test. TEG supply is 3.6V DC supply.

histogram display, and built-in machine vision code examples [66]. Using OpenMV IDE, we build a dataset and upload it to Edge Impulse [67] in the cloud. We used transfer learning with MobileNetV2 to generate a TensorFlow Lite Convolutional Neural Network (CNN) that runs on board with the OpenMV Cam H7 Plus camera. A step-by-step tutorial on how to do image classification using OpenMV IDE and Edge Impulse can be found in these links: [68] and [69].

### III. EVALUATION OF RESULTS

Without the silicone material, the machine vision camera can be used for the usual applications of capturing images. By combining the flexible material with reflective coating with a machine vision camera, the setup becomes a compact and unified visuotactile sensor that can be used for tactile

forces analysis and image classification. We improved the reflective coating that we introduced in our previous studies [34], [45] by adding thermosensitive reflective layers on top of the switchable UV markers. Activated UV markers are shown in Fig. 7(d).

#### A. Temperature Sensing

We evaluated our sensor using TEG TES1-03102  $15\text{ mm} \times 15\text{ mm}$  Peltier Thermo Electric Generator (TEG). We performed a temperature sweep test and sensor response time test. Details on these two tests are discussed in the following sections.

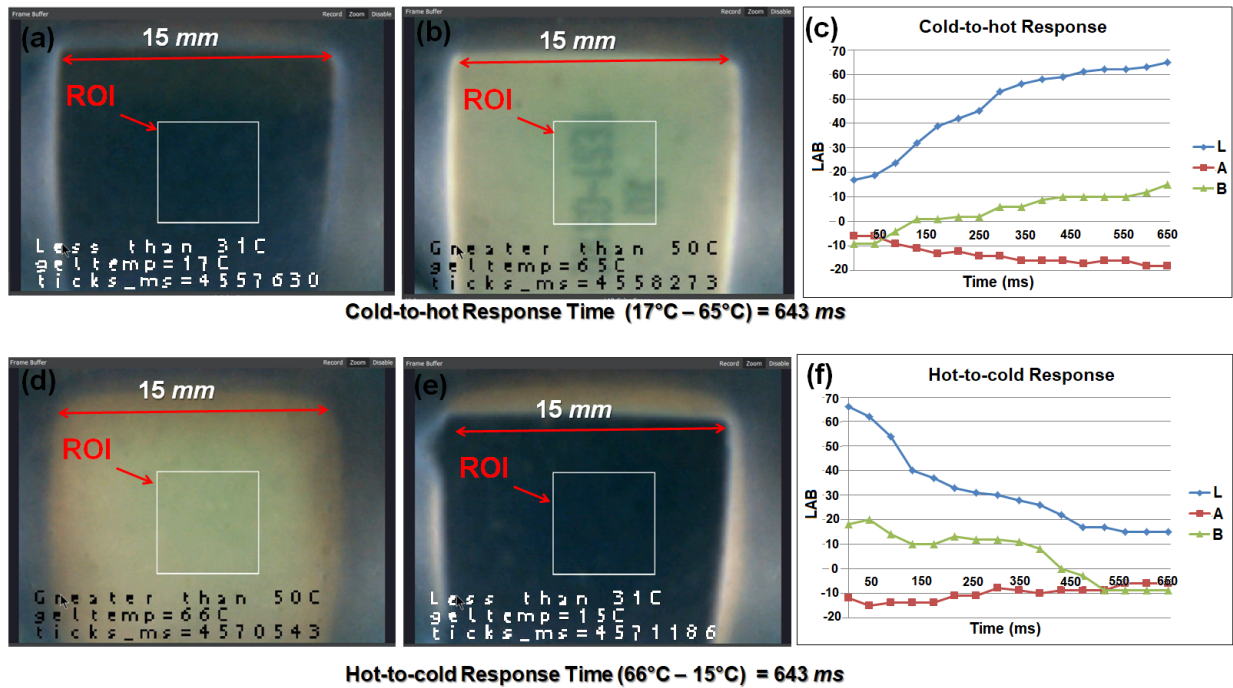


**Fig. 11.** Response time. (a) The cold plate of TEG shows a dark blue color when pressed to the sensor indicating below the 31°C threshold of the blue thermochromic pigment. (b) When the TEG was flipped pressing the hot-side to the sensor, the reflective layer changes to semi-transparent indicating that the 50°C pigment threshold has been exceeded. The part name of the TEG can be seen when all the temperature thresholds have been reached as shown in Fig. 11(b). The response graph of cold-to-hot is shown in Fig. 11(c). Moreover, hot to cold response time pictures can be seen from Fig. 11(d) and Fig. 11(e) respectively and hot-to-cold data were plotted as shown Fig. 11(f). The ticks.ms is the machine time in milliseconds showing the elapsed time between two events. The rest of the color changes can be found in a test video here [57].

### 1) Temperature sweep

We used a 2.4V DC power supply using two rechargeable dry cells to heat the TEG slowly. Using two identical TEGs, one has a thermistor and the other connected to our sensor, we recorded the temperature reading and the LAB mode values, respectively, as the TEGs temperature rises. The temperature sweep time took 23 s from 23°C to greater than 55°C.

The temperature test results captured by our sensor are shown in Fig. 8. As the temperature increases, the color of the reflective coating changes. The rest of the color changes can be found in a test video here [57]. The camera captures the color change in the reflective coating and with the use of image processing, we can infer the temperature of the contacted object. The colors of an image can be analyzed using different color spaces such as Red-Green-Blue (RGB), Hue-Saturation-Value (HSV), and Lightness\*a\*b\* (LAB). The finger-shaped GelForce that can sense temperature [25], [26] and the thermosensitive visuotactile sensor in our previous study [46] used the HSV color space and OpenCV library that has a builtin function that can easily access the HSV values of a given Region-Of-Interest (ROI). In this study, the machine vision camera we used processes image data in LAB color space instead of HSV. The 'L' is the lightness value ranging from 0 (black) to 100 (white), 'A' is the green-red axis ranging from -128 to +128, and 'B' is the blue-yellow axis ranging from -128 to +128 [70], [71]. The lightness value in the LAB color space is the amount of white or black within a given hue. We defined an ROI demarcated by a white line as shown in Fig. 8 and Fig. 11 and recorded the L, A, and B

mode values or the dominant color values in the LAB color space within the ROI. The ROI area can be changed and move across the frame to select the part of the tactile image where the temperature is to be measured. In this study, we fixed the position of the ROI in the middle of the frame. Knowing the temperature threshold of thermochromic pigments, we can estimate the temperature of the object or on which temperature range it belongs as it touches our sensor. We recorded the L, A, B mode values and superimposed the thermistor temperature reading as shown in Fig. 9. It was reported in [26] that in order for them to cover 15–45°C, the researchers have to use several thermosensitive paints that have different temperature ranges but their prototype has thermal measurement results range of 32°C–35°C only, similar to [25]. Whereas our sensor range goes from 31°C–50°C.

Our sensor's response graph, as shown in Fig. 9, presents the temperature, and 'L' or the lightness value in the LAB color space has direct proportionality with temperature change, which can be used to estimate the temperature of the object touching our sensor within the temperature range of 31°C–50°C where 'L' has a linear relationship with temperature and also corresponds to the minimum and maximum temperature thresholds of the thermosensitive pigments of our sensor. Our sensor has a wider temperature measurement range of 31°C - 50°C as compared to the 32°C - 35°C range of finger-shaped GelForce [25], [26]. Instead of relating temperature as a function of hue like in our previous pilot study [46], and finger-shaped GelForce, we relate our sensor's temperature measurement to the lightness value ('L') captured by

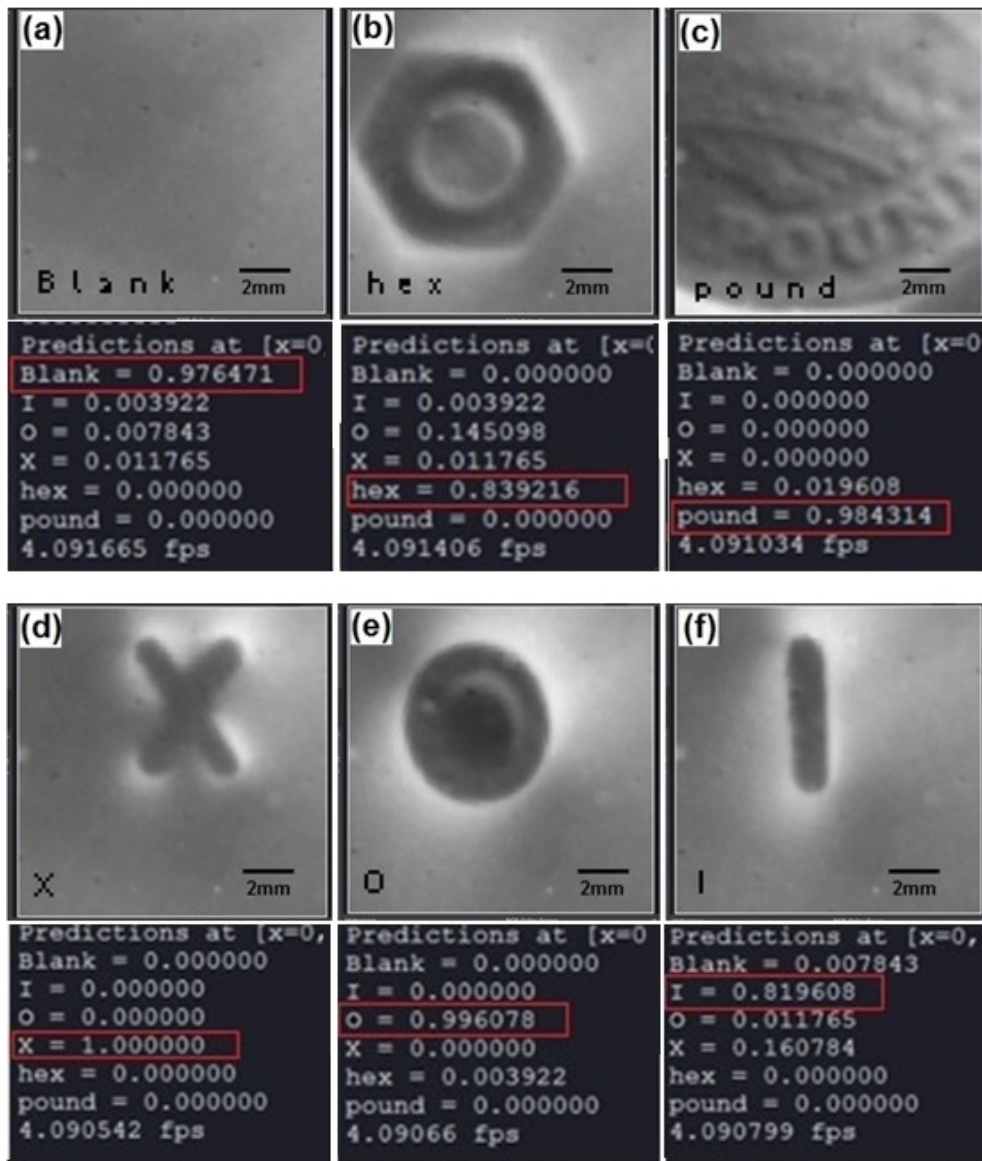


Fig. 12. Classification results using the OpenMV Cam H7 Plus camera: a) blank result when there is no object touching the sensor, b) hex end of a precision screwdriver, c) back of UK one-pound coin, and the letters X, O, I letters from a cookie stamp are shown in d), e), and f) respectively. The prediction results are shown below of each tactile image.

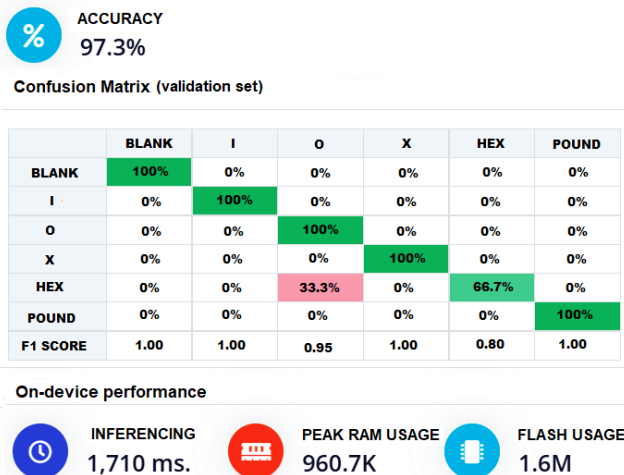


Fig. 13. Confusion Matrix and On Device Performance produced by Edge Impulse.

our machine vision camera, as shown in Fig. 9. Thus, we write the temperature measurement equation of our sensor as temperature ( $T$ ) as a function of lightness ( $L$ ), as shown in Eq. (1).

$$T = f(L) \tag{1}$$

2) *Response time*

By supplying a 3.6V DC supply to the TEG, it heats up faster compared to a 2.4V DC supply covering the same span of L mode values in just 6.5 s instead of 23 s as shown in Fig. 10. The thermistor has a slower response compared to our sensor. The epoxy encapsulated NTC thermistor, similar to what we used in the testing, has a response time of 19.54 s for temperature change 25°C to 41°C based on this report [72]. We quantified the response time of our sensor by flipping the TEG’s hot and cold plates and recording the time on which our sensor’s reflective layer changes from blue to

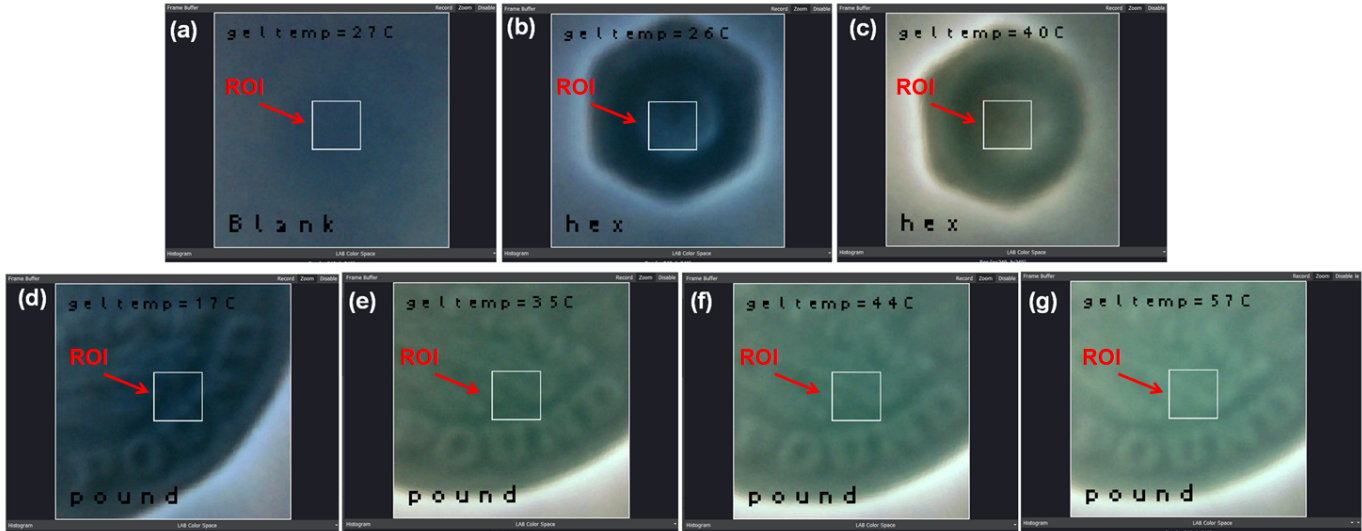


Fig. 14. Combined temperature sensing and image recognition test. Temperature reading and image recognition result is shown simultaneously. (a) Blank or no object is pressed on the sensor, (b) a cold end of a hex screwdriver, (c) a hot end of hex screwdriver heated using TEG, (d) a cold UK one-pound coin that has less than 31°C is pressed to the sensor, (e) the coin is heated using TEG and the coin temperature is within 31°C-43°C, (f) coin temperature is within 43°C-50°C, and (g) coin temperature is greater than 50°C.

transparent. The “ticks\_ms” in Fig. 11 is the machine time in milliseconds showing the elapsed time between two events. We were able to measure a response time of 643 ms for cold-to-hot and hot-to-cold. The rapid temperature response of our visuotactile sensor is comparable to the less than one second time withdrawal reflex response of the human autonomic system to extreme heat [73]. Our sensor might give robots the ability to react as humans and create thermosensitive soft robots in the near future. The response time results of our sensor are shown in Fig. 11. The response time test covers the minimum thermochromic pigment threshold of 31°C until the highest thermochromic pigment threshold of 50°C. The dark blue color in the ROI, as shown in Fig. 11(a) and Fig. 11(e), indicates that the blue thermochromic pigment is not activated, and the temperature of TEG is less than the 31°C temperature threshold of the blue thermochromic pigment. Moreover, Fig. 11(b) and Fig. 11(d) show that the thermochromic pigment with a 50°C threshold has been activated making the reflective layer of our sensor translucent. The rest of the color changes can be found in a test video here [57].

### 3) Calibration

Based on the graph shown in Fig. 9, the ‘L’ is directly proportional to the temperature reading of the thermistor. By knowing the thermochromic pigment temperature thresholds, we subtracted offset values to make the ‘L’ linearity graph coincides with the thermistor response graph. The “geltemp” reading in Fig. 8 is the corrected ‘L’ value of our sensor corresponding to the thermistor reading. Maximum geltemp deviation relative to the thermistor reading within 31°C-50°C range is 3.75°C near the 31°C pigment threshold.

Knowing that the temperature and lightness value has a linear relationship within the temperature range of 31°C-50°C, we can write the calibration equation as

$$T = mL \pm C \quad (2)$$

where ( $T$ ) is temperature, ( $m$ ) is the slope, ( $L$ ) is the lightness value, and ( $C$ ) is the offset value.

### B. Image Recognition

Using Edge Impulse and by following the video tutorial given in [69], we were able to collect different tactile images for our dataset, how to apply transfer learning to train a neural network, and deploy the system to our OpenMV Cam H7 Plus camera. We used MobileNetV2 0.35 that uses around 296.8K RAM and 575.2K ROM with default settings and optimizations. This model works best with a 96x96 input size and supports both RGB and grayscale images. We used 20 training cycles during the transfer learning, 10 neurons in the final layer. After transfer learning, we deployed the model to our machine vision camera. According to [69], 30 images are sufficient, yet we collected 40 image samples from each of the five different objects: UK one-pound coin, hex end of a precision screwdriver, and I, O, and X letters from a cookie stamp. We also collected 40 images of the blank screen when there is no object being touched by the sensor. We captured a total of 240 images and uploaded them to Edge Impulse cloud, which automatically divided them into 182 training samples and 58 testing samples. The results of our tactile image classification done using our machine vision camera are shown in Fig. 12. The prediction results are on the top of each tactile image.

After we processed all our data, we trained the neural network using transfer learning. We used MobileNetV2 available in Edge Impulse and achieved 97.3% accuracy during testing. There was an error in classifying a ‘hex’ as an ‘o’. The confusion matrix is shown in Fig. 13. Besides the confusion matrix is the on-device performance measured on the OpenMV Cam H7 Plus camera. The Edge Impulse makes a complete package of the trained model ready to be deployed on a machine vision camera.

### C. Combined Image Recognition and Temperature Test

Image recognition and temperature test can be done separately as discussed in sections III.A. and III.B. but can also be done simultaneously. We developed a unified application that combined the algorithms for image recognition and temperature sensing giving image classification and temperature measurement results simultaneously in one image frame when the sensor is contacted by an object. In the combined test, we recorded the gel temperature when no object was pressed to our sensor. The image recognition algorithm displays a ‘Blank’ result together with the gel temperature in the display image frame, as shown in Fig. 14a. We pressed the cold end of a hex screwdriver and the cold UK one-pound coin to our sensor and recorded the results. We then heated the end of a hex screwdriver, and UK one-pound coin using the TEG, and pressed each one to the sensor. We did a cold and hot test for the end of the hex screwdriver and a gradient temperature test for the coin covering all the thresholds of layered thermochromic pigments. The combined temperature and image recognition test results are shown in Fig. 14.

### D. WiFi Connection

Using the OpenMV WiFi module [74], the OpenMV Cam H7 Plus camera can communicate wirelessly. It uses ATWINC1500 network controller. Images in grayscale as shown in Fig. 15(a) and RGB, as shown in Fig. 15(b), can be transmitted via WiFi. There are two modes of operations: 1) station mode, which is the default mode wherein the module connects to an access point as a client, and b) the Access Point (AP) mode wherein the module acts as a hotspot and can accept connection from a client. The available WiFi hotspots during the station mode scanning test of our machine vision camera are shown in Fig. 15(c), and the IP address and the OPENMV\_AP AP mode connection properties are shown in Fig. 15(d). A video tutorial on how to configure as an access point can be found in [75].

## IV. CONCLUSION AND RECOMMENDATION

In this study, we presented a compact, GelSight-like sensor with temperature sensing capability by using thermochromic pigments in the reflective layer. Three layers of thermochromic pigments with different colors and thresholds were painted on one side of a clear low-cost, commercially available cosmetic silicone sponge to make the reflective layer thermosensitive. An OpenMV Cam H7 plus camera was used to record the LAB mode values, and classify or recognize different tactile images. Our test results show that the ‘L’ mode value in the LAB color space recorded by our machine vision camera shows a linear relationship with temperature. Moreover, we were able to measure a response time of 643 *ms* for the cold-to-hot and hot-to-cold response that covers 31°C to 50°C. Moreover, our novel visuotactile sensor is capable of detecting a rapid temperature changes (30°C/s). This feature could be useful for soft robots to act equivalent to humans’ withdrawal reflex in touching hot surfaces in search and rescue, industrial applications, and space explorations. Furthermore, this next generation thermosensitive visuotactile sensor would be useful

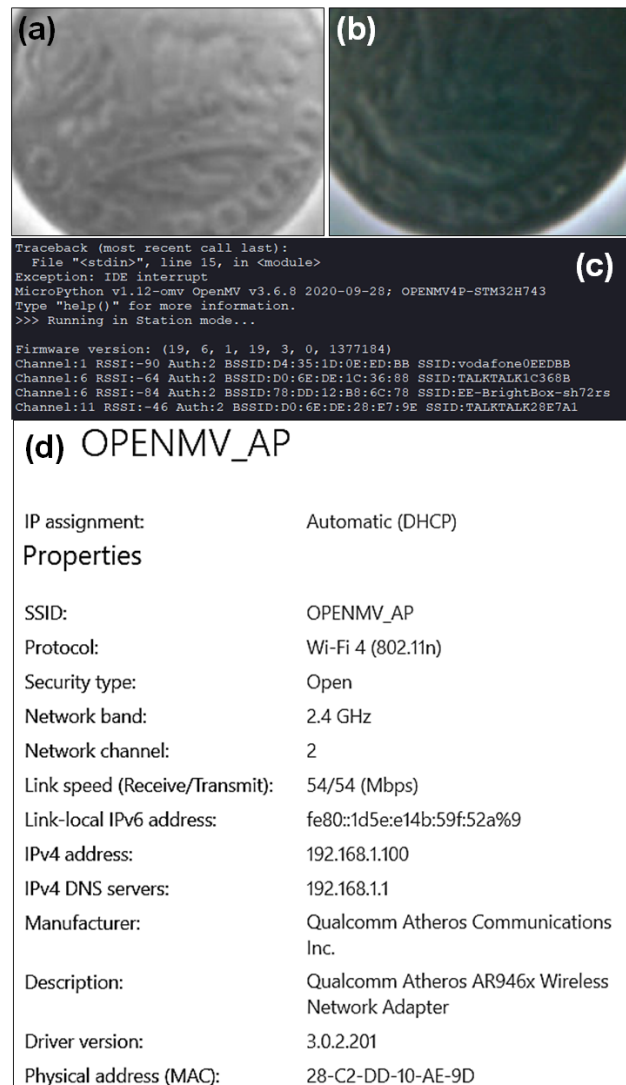


Fig. 15. Station mode, and AP mode WiFi connections. Images in grayscale as shown in Fig. 15(a) and RGB as shown in Fig. 15(b) can be transmitted via WiFi. The available WiFi during station mode scanning test are shown in Fig. 15(c), and the IP address and the OPENMV\_AP AP mode connection properties are shown in Fig. 15(d).

in future research on 3D image reconstruction in perception not only haptic-based primary colors (force, vibration, and temperature). Using the OpenMV Cam H7 plus machine vision camera, a trained MobileNetV2 model using Edge Impulse was deployed to it. A high success rate of 97.3% classification accuracy on five different objects using their tactile images was achieved in spite of a small dataset. This study demonstrated that the current GelSight sensor technology could be improved by providing temperature sensing capability using thermochromic pigments on the reflective coating, onboard tactile image classification, and wireless connectivity using a OpenMV Cam H7 camera all in one sensor module.

### ACKNOWLEDGMENT

The authors would like to thank Liverpool Hope University, De La Salle University, Manila, and DOST-ERDT for helping them in this study.

## REFERENCES

- [1] J. R. Anshel, "Visual ergonomics in the workplace," *Aaohn Journal* 55, 10 (2007), 414–420
- [2] A. Ranasinghe, N. Sornkarn, P. Dasgupta, K. Althoefer, J. Penders, T. Nanayakkara, "Salient Feature of Haptic-Based Guidance of People in Low Visibility Environments Using Hard Reins," *IEEE Transactions on Cybernetics*, vol. 46, no. 2, pp. 568–579, 2016.
- [3] M. J. Morgan, "Molyneux's Question: Vision, Touch and the Philosophy of Perception," Cambridge: Cambridge University Press, 1977. <https://repository.upenn.edu/dissertations/AAI13808064>
- [4] S. Luo, J. Bimbo, R. Dahiya, H. Liu, "Robotic Tactile Perception of Object Properties: A Review," *Mechatronics*, 48, 54–67, 2017.
- [5] W. Li, Y. Noh, A. Alomainy, I. Vitanov, Y. Zheng, P. Qi, K. Althoefer, "F-TOUCH Sensor for Three-Axis Forces Measurement and Geometry Observation," 2020 IEEE SENSORS, 2020, pp. 1–4, doi: 10.1109/SENSORS47125.2020.9278600.
- [6] R. Calandra, A. Owens, D. Jayaraman, W. Yuan, J. Lin, J. Malik, E. H. Adelson, and S. Levine, "More than a feeling: Learning to grasp and regrasp using vision and touch," *IEEE Robotics and Automation Letters (RA-L)*, 2018.
- [7] A. C. Abad and A. Ranasinghe, "Visuotactile Sensors with Emphasis on GelSight Sensor: A Review", *IEEE Sensors Journal*, DOI: 10.1109/JSEN.2020.2979662
- [8] J. Chodera, "Examination methods of standing in man," *FU CSA VPraha.*, 1957, vols. I-III.
- [9] J. Chodera, "Pedobarograph - apparatus for the visual demonstration of the clinging surfaces of the irregularly shaped objects," 1960, *Czs Patent* 104 514 30d.
- [10] J. D. Chodera, M. Lord, "Pedobarographic Foot — Pressure Measurements and Their Applications," In: Kenedi R.M., Paul J.P., Hughes J. (eds) *Disability. Strathclyde Bioengineering Seminars*. Palgrave Macmillan, London, 1979.
- [11] L. Klenerman, B. Wood, "The Measurement of Footprints (Pedobarography)," In: *The Human Foot*. Springer, London, 2006.
- [12] T. G. Strickler, "Design of an Optical Touch sensing system for a remote manipulator," MIT Mechanical Engineering Masters Thesis, June, 1966. <https://dspace.mit.edu/handle/1721.1/13413>
- [13] J. L. Schneiter, T.B. Sheridan, "An optical tactile sensor for manipulators," *Robotics and Computer Integrated Manufacturing*, Vol.1, No.1, pp.65–71, 1984.
- [14] K. Tanie, K. Komoriya, M. Kaneko, S. Tachi, and A. Fujikawa, "A high resolution tactile sensor," *Proceedings of the 4th International Conference on Robot Vision and Sensory Controls*, pp.251–260., October 1984.
- [15] H. Hiraishi, N. Suzuki, M. Kaneko, K. Tanie, "An Object Profile Detection by a High Resolution Tactile Sensor Using an Optical Conductive Plate," *Proc. of IECON '88 14th Annual Conf. of IEEE Industrial Electronics Society*, pp. 982–987, 1988.
- [16] S. Begej, "Planar and finger-shaped optical tactile sensors for robotic applications," *IEEE J. Robotics Autom.*, vol. 4, no. 5, pp. 472–484, Oct. 1988.
- [17] N. Nakao, M. Kaneko, N. Suzuki, K. Tanie, "A Finger Shaped Tactile Sensor Using an Optical Waveguide," *Proc. of IECON '90 16th Annual Conf. of IEEE Industrial Electronics Society*, pp. 300–305, 1990.
- [18] H. Maekawa, K. Tanie, "Development of a miniaturized model of a finger shaped tactile sensor using an optical waveguide," *Proc. of 17th Annual Conf. of IEEE Industrial Electronics Society*, 1991.
- [19] H. Maekawa, K. Tanie, K. Komoriya, M. Kaneko, C. Horiguchi, T. Sugawara, "Development of a Finger-Shaped Tactile Sensor and its Evaluation by Active Touch," *Proc. of IEEE Int. Conf. on Robotics and Automation*, pp. 1327–1334, 1992.
- [20] M. Ohka, Y. Mitsuya, S. Takeuchi, O. Kamekawa, "A Three-axis Optical Tactile Sensor (FEM Contact Analyses and Sensing Experiments Using a Large-sized Tactile Sensor)," *Proc. 1995 IEEE Int. Conf. on Robotics Automation*, pp. 817–824, 1995.
- [21] M. Ohka, Y. Mitsuya, K. Hattori, I. Higashioka, "Data Conversion Capability of Optical Tactile Sensor Featuring an Array of Pyramidal Projections," *Proc. 1996 IEEE/SICE/RJS Proc. Int. Conf. on Multisensor Fusion and Integration for Intelligent Systems*, pp. 573–580, 1996.
- [22] C. Chorley, C. Melhuish, T. Pipe, and J. Rossiter, "Development of a Tactile Sensor Based on Biologically Inspired Edge Encoding," *Design*, 2008.
- [23] D. Hristu, N. Ferner, R.W. Brockett, "The performance of a deformable-membrane tactile sensor: basic results on geometrically-defined tasks." *Proc. IEEE Int'l Conf. on Robotics and Automation*, 2000
- [24] K. Kamiyama, H. Kajimoto, M. Inami, N. Kawakami, S. Tachi, "A Vision-based Tactile Sensor," *International Conference on Artificial Reality and Telexistence*, 2001.
- [25] K. Sato, H. Shinoda, S. Tachi, "Vision-based cutaneous sensor to measure both tactile and thermal information for telexistence," *Proc. 2011 IEEE International Symposium on VR Innovation*, pp. 119–122, 2011.
- [26] K. Sato, H. Shinoda and S. Tachi, "Finger-shaped thermal sensor using thermo-sensitive paint and camera for telexistence," 2011 IEEE International Conference on Robotics and Automation, 2011, pp. 1120–1125, doi: 10.1109/ICRA.2011.5980271.
- [27] C. Sferrazza, R. D'Andrea, "Design, Motivation and Evaluation of a Full-Resolution Optical Tactile Sensor," *Sensors* 2019, 19, 928.
- [28] X. Lin, M. Wiertelowski, "Sensing the Frictional State of a Robotic Skin via Subtractive Color Mixing," *IEEE Robotics and Automation Letters (RAL)* paper presented at the 2019 International Conference on Robotics and Automation (ICRA) Palais des congrès de Montreal, Montreal, Canada, May 20–24, 2019
- [29] M. K. Johnson and E. Adelson, "Retrographic sensing for the measurement of surface texture and shape," in *Computer Vision and Pattern Recognition (CVPR)*, 2009 IEEE Conference on. IEEE, 2009, pp. 1070–1077.
- [30] M. K. Johnson, F. Cole, A. Raj, and E. H. Adelson, "Microgeometry capture using an elastomeric sensor," in *TOG*, vol. 30, no. 4. ACM, 2011, p. 46.
- [31] R. Li and E. Adelson, "Sensing and recognizing surface textures using a gelsight sensor," in *Proceedings of the IEEE Conference on Computer Vision and Pattern Recognition*, 2013, pp. 1241–1247.
- [32] X. Jia, R. Li, M. A. Srinivasan, and E. H. Adelson, "Lump detection with a gelsight sensor," in *World Haptics Conference (WHC)*, 2013. IEEE, 2013, pp. 175–179.
- [33] R. Li, R. Platt, W. Yuan, A. ten Pas, N. Roscup, M. A. Srinivasan, and E. Adelson, "Localization and manipulation of small parts using gelsight tactile sensing," in *Intelligent Robots and Systems (IROS 2014)*, 2014 IEEE/RJS International Conference on. IEEE, 2014, pp. 3988–3993.
- [34] A. C. Abad, A. Ranasinghe, "Low-cost GelSight with UV Markings: Feature Extraction of Objects Using AlexNet and Optical Flow without 3D Image Reconstruction", *International Conference on Robotics and Automation (ICRA2020)*, May 31 - June 4, 2020, Palais des Congrès de Paris, France.
- [35] W. Yuan, "Tactile measurement with a gelsight sensor," Master's thesis, MIT, Cambridge, MA, USA, 2014.
- [36] W. Yuan, S. Dong, and E. H. Adelson, "GelSight: High resolution robot tactile sensors for estimating geometry and force," *Sensors*, vol. 17, no. 12, p. 2762, 2017.
- [37] M. Bauza, O. Canal and A. Rodriguez, "Tactile Mapping and Localization from High-Resolution Tactile Imprints," 2019 International Conference on Robotics and Automation (ICRA) Palais des congrès de Montreal, Montreal, Canada, May 20–24, 2019, pp. 3811–3817.
- [38] S. Dong, W. Yuan, and E. Adelson, "Improved GelSight tactile sensor for measuring geometry and slip," *IROS*, 2017.
- [39] E. Donlon, S. Dong, M. Liu, J. Li, E. Adelson, A. Rodriguez, "Gel-Slim: A High-Resolution, Compact, Robust, and Calibrated Tactile-sensing Finger," *IROS 2018*: 1927–1934.
- [40] W. Yuan, R. Li, M. A. Srinivasan, and E. H. Adelson, "Measurement of shear and slip with a gelsight tactile sensor," in *Robotics and Automation (ICRA)*, 2015 IEEE International Conference on. IEEE, 2015, pp. 304–311.
- [41] J. Li, S. Dong, E. Adelson, "Slip Detection with Combined Tactile and Visual Information," *ICRA 2018*: 7772–7777, arXiv:1802.10153.
- [42] W. Yuan, Y. Mo, S. Wang, E. H. Adelson, "Active Clothing Material Perception Using Tactile Sensing and Deep Learning," *ICRA 2018*: 1–8.
- [43] J. Lee, D. Bollegala, S. Luo, " "Touching to See" and "Seeing to Feel": Robotic Cross-modal Sensory Data Generation for Visual-Tactile Perception," 2019 International Conference on Robotics and Automation (ICRA) Palais des congrès de Montreal, Montreal, Canada, May 20–24, 2019, pp. 4276–4282.
- [44] S. Luo, W. Yuan, E. Adelson, A. Cohn and R. Fuentes, "ViTac: Feature Sharing between Vision and Tactile Sensing for Cloth Texture Recognition", *IEEE International Conference on Robotics and Automation (ICRA)*, 2018
- [45] A. C. Abad, D. Reid, A. Ranasinghe, "Pilot Study: Low Cost Gel-Sight Sensor," *Workshop on ViTac: Integrating Vision and Touch for Multimodal and Cross-modal Perception*, *ICRA 2019 ViTac Workshop* Accepted paper, <http://wordpress.csc.liv.ac.uk/smartlab/icra-2019-vitac-workshop-accepted-papers/>

- [46] A. C. Abad, M. Ormazabal, D. Reid, A. Ranasinghe, "Pilot Study: A Visuotactile Haptic Primary Colors Sensor", 2021 IEEE SENSORS, Virtual Conference Oct. 31-Nov. 4, 2021.
- [47] R. Li, "Touching Is Believing: Sensing and Analyzing Touch Information with GelSight," Ph.D. Thesis, Massachusetts Institute of Technology, Cambridge, MA, USA, 2015.
- [48] W. Li, J. Konstantinova, Y. Noh, A. Alomainy, K. Althoefer, "Camerabased force and tactile sensor." Towards Autonomous Robotic Systems: 19th Annual Conference, TAROS 2018, Bristol, UK July 25-27, 2018, Proceedings. Vol. 10965 LNAI, pp. 438-450.
- [49] What is silicone rubber?, Available online: <https://www.smooth-on.com/support/faq/198/> (accessed on 2 August 2021)
- [50] GelSight. Available online: <https://www.youtube.com/watch?v=aKoKVA4Vcu0> (accessed on 2 August 2021)
- [51] S. Tachi, K. Minamizawa, M. Furukawa and C. L. Fernando, "Haptic media construction and utilization of human-harmonized "tangible" information environment," 2013 23rd International Conference on Artificial Reality and Telexistence (ICAT), 2013, pp. 145-150, doi: 10.1109/ICAT.2013.6728921.
- [52] OpenMV Cam H7 Plus. Available online: <https://openmv.io/products/openmv-cam-h7-plus> (accessed on 2 August 2021)
- [53] Liquid Crystal Thermochromic Colour Changing Sheet. Available online: <https://www.sfxco.co.uk/products/lc-liquid-crystal-thermochromic-sheets?variant=6780064833> (accessed on 2 August 2021)
- [54] SFXC® SPRAYABLE LIQUID CRYSTAL INK. Available online: <https://www.sfxco.co.uk/products/sprayable-liquid-crystal-inks> (accessed on 2 August 2021)
- [55] COLOUR CHANGING THERMOCHROMIC PIGMENT TRIAL PACK - COLOUR TO COLOUR. Available online: <https://www.sfxco.co.uk/collections/thermochromatic-thermochromic-pigments-ink-paint/products/colour-changing-thermochromic-pigment-trial-pack> (accessed on 2 August 2021)
- [56] Thermochromic pigment. Available online: <https://www.aliexpress.com/store/2071018?spm=a2g0o.detail.1000002.2.2ef28326dujrbt> (accessed on 2 August 2021)
- [57] HaptiTemp videos. Available online: <https://drive.google.com/drive/u/1/folders/1fS1P-nl0cHBa3WUsWQFPRBCXzJ9TW59p> (accessed on 2 August 2021)
- [58] K. Shimonomura, "Tactile Image Sensors Employing Camera: A Review," *Sensors* 19(18): 3933 (2019)
- [59] Sipeed MAix Go. Available online: <https://www.seeedstudio.com/Sipeed-MAix-GO-Suit-for-RISC-V-AI-IoT-p-2874.html> (accessed on 2 August 2021)
- [60] M5StickV. Available online: <https://m5stack.com/products/stickv> (accessed on 2 August 2021)
- [61] Kittenbot KOI AI. Available online: <https://www.kittenbot.cc/products/kittenbot-koi-artificial-intelligence-module> (accessed on 2 August 2021)
- [62] Jevois Smart Machine Vision Camera. Available online: <http://jevois.org/> (accessed on 2 August 2021)
- [63] HUSKYLENS: AI Camera with Kendryte K210. Available online: <https://community.dfrobot.com/makelog-308252.html> (accessed on 2 August 2021)
- [64] Google AIY Vision Kit. Available online: <https://aiyprojects.withgoogle.com/vision> (accessed on 2 August 2021)
- [65] OpenCV AI Kit: OAK—1. Available online: <https://store.openai.com/products/oak-1> (accessed on 2 August 2021)
- [66] OpenMV IDE. Available online: <https://openmv.io/pages/download> (accessed on 2 August 2021)
- [67] Edge Impulse. Available online: <https://www.edgeimpulse.com/> (accessed on 2 August 2021)
- [68] Smile Detection with OpenMV IDE and Edge Impulse. Available online: <https://www.youtube.com/watch?v=YKwVope5RsU&feature=youtu.be> (accessed on 2 August 2021)
- [69] Adding sight to your sensors. Available online: <https://docs.edgeimpulse.com/docs/image-classification> (accessed on 2 August 2021)
- [70] A. Delazio, A. Israr and R. L. Klatzky, "Cross-modal correspondence between vibrations and colors," 2017 IEEE World Haptics Conference (WHC), 2017, pp. 219-224, doi: 10.1109/WHC.2017.7989904.
- [71] OpenMV MicroPython libraries. Available online: <https://docs.openmv.io/library/omv.image.html> (accessed on 2 August 2021)
- [72] M. Samii, "Understanding, Measuring, And Using Thermistor Thermal Time Constants", Feb 24, 2017. Available online: <https://www.fierceelectronics.com/components/understanding-measuring-and-using-thermistor-thermal-time-constants> (accessed on 2 August 2021)
- [73] J.M. Castellote, J. Valls-Solé, "Temporal relationship between perceptual and physiological events triggered by nociceptive heat stimuli," *Sci Rep* 9, 3264 (2019). <https://doi.org/10.1038/s41598-019-39509-3>
- [74] OpenMV WiFi Shield. Available online: <https://openmv.io/products/wifi-shield-1> (accessed on 2 August 2021)
- [75] SingTown - OpenMV Cam video tutorial 12 - WiFi Shield. Available online: <https://www.youtube.com/watch?v=wIwJhw2rBkQ&t=329s> (accessed on 2 August 2021)



**Alexander C. Abad** (Member, IEEE) received the B.S. degree in Electronics and Communications Engineering (ECE) from St. Louis University, Baguio City, Philippines, in 2002, and the M.S. degree in ECE from De La Salle University, Manila, Philippines, in 2011. He is currently pursuing the Ph.D. in Computer Science and Informatics at Liverpool Hope University, U.K. His research interests include robotics, haptics, machine intelligence, machine vision, mixed-signal electronics, and IC design.



**David Reid** (Member IEEE) has a Ph.D. from Liverpool University in Computer Science in 1995. This work involved research into intelligent browsing categorisation. He later joined a newly formed group at Liverpool University dedicated to developing and promoting innovative technological solutions. After implementing the first electronic shopping mall in the U.K., he spent eight years providing technical leadership on many Internet and Intranet projects. These projects usually involved exploiting newly emergent technology. His current research interests are derived from experience gained in both in academic and industrial backgrounds, and include: AI, Augmented and Virtual Reality and Spatial Computing.



**Anuradha Ranasinghe** (Member, IEEE) received the BSc in Physics from University of Sri Jayewardanapura, Sri Lanka and the Ph.D. degree in Robotics from King's College London, London, U.K in 2015. She is currently a Lecturer of Robotics with Liverpool Hope University, Liverpool, U.K.

Her current research interests include tactile-based miniaturized sensors for engineering and medical applications, humans' perception, and haptics. Her work on human-robot interactions was featured in EPSRC news release and California based CBS Radio in a live interview. Moreover, her recent work on miniaturized haptic-based sensors was featured in Liverpool Echo, Manchester evening news, North Wales live, and Belfast live. Her work was accepted for a finalist for the IEEE Franklin V. Taylor memorial award for the best paper in the IEEE Systems, Man, and Cybernetics conference, Manchester, UK in 2013.